

## Barriers to Rotation of Axially Coordinated Imidazole Ligands in Nonplanar *meso*-Tetraalkylporphyrinato-cobalt(III) Complexes

Takashi Saitoh, Takahisa Ikeue, Yoshiki Ohgo, and Mikio Nakamura\*,

Contribution from the Department of Chemistry, Toho University School of Medicine, Omorinishi, Ota-ku, Tokyo 143

**Abstracts.** Dynamic NMR study of a series of *meso*-[Co(TRP)(L)<sub>2</sub>]Cl, where R is an alkyl group and L is a substituted imidazole, has been carried out. While the complexes with unhindered imidazole show no splitting of the signals, those with bulky imidazoles exhibit change in line shape, indicating the hindered imidazole rotation. The activation free energy increases as R and/or L become bulkier. Based on the red-shifted Soret and Q bands in the UV-Visible and the downfield shifted imidazole protons in the <sup>1</sup>H NMR spectra of these complexes as compared with the *meso* unsubstituted complexes, it is concluded that the deformation of the porphyrin ring slows down the rate of rotation of the coordinated ligand. © 1997 Elsevier Science Ltd.

### INTRODUCTION

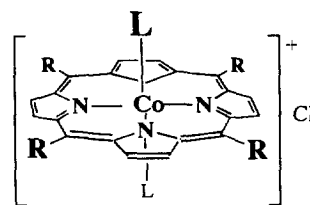
The orientation effect of the axially coordinated imidazole ligands on the heme properties have been the subject of increasing study in connection with the biological system where the coordinated ligand is tightly fixed in the cavity of heme protein.<sup>1-5</sup> Some years ago, we have reported the first example of the hindered rotation of axially coordinated 2-methylimidazole(2-MeIm) in *meso*-tetramesitylporphyrinatoiron(III), [Fe(TMP)(2-MeIm)<sub>2</sub>]Cl.<sup>6</sup> This complex showed a pyrrole signal at a very high field,  $\delta$  -10.8 ppm at 25 °C, which split into four signals at  $\delta$  -14.7, -19.0, -21.0, and -23.3 ppm, at -56 °C. The result was interpreted in terms of the fixation of the coordinated 2-MeIm ligand on the NMR time scale due to the hindered rotation about iron-nitrogen bonds. The activation free energy for the ligand rotation was 50 kJ mol<sup>-1</sup> at -22 °C. The frozen conformation in solution was determined to be the one where the coordinated imidazole ligands are placed along the diagonal C<sub>meso</sub>-Fe-C<sub>meso</sub> axes, perpendicularly to each other.<sup>7,8</sup> The structure was further supported by the X-ray crystallographic analysis of the analogous [Fe(TMP)(1,2-Me<sub>2</sub>Im)<sub>2</sub>]ClO<sub>4</sub>.<sup>9</sup> The porphyrin ring of this complex showed a highly S<sub>4</sub>-ruffled structure where the average deviation of the four *meso* carbons from the mean porphyrin plane reached as much as 0.72 Å. This indicates that the complex has two cavities developed along the diagonal C<sub>meso</sub>-Fe-C<sub>meso</sub> axes and that the coordinated imidazole ligands are placed in the cavities perpendicularly to each other. Thus, the solid structure is maintained even in solution.

Recently, we have reported another iron porphyrin system in which rotation of the coordinated 2-MeIm is hindered on the NMR time scale.<sup>10</sup> They are a series of bis(2-methylimidazole)(*meso*-tetraalkylporphyrinato-iron(III)) complexes [Fe(TRP)(2-MeIm)<sub>2</sub>]Cl (R = Me, Et, and <sup>i</sup>Pr). While the unsubstituted complex [Fe-(THP)(2-MeIm)<sub>2</sub>]Cl showed no signal splitting even at -72 °C, the pyrrole and the *meso*  $\alpha$ -proton signals of the methyl complex [Fe(TMeP)(2-MeIm)<sub>2</sub>]Cl started to split below -51 °C and showed four signals ( $\delta$  -6.3, -11.3, -14.4, and -15.5 ppm) for the pyrrole and two signals ( $\delta$  39.0 and 49.6 ppm) for the *meso* methyl

protons at  $-71\text{ }^{\circ}\text{C}$ . The splitting patterns of the pyrrole and *meso*-methyl signals clearly indicate that the stable conformation is the same as that in  $[\text{Fe}(\text{TMP})(2\text{-MeIm})_2]\text{Cl}$ . The activation free energy for ligand rotation was determined to be  $40\text{ kJ mol}^{-1}$  at  $-51\text{ }^{\circ}\text{C}$ . The signal splitting of the methyl complex was quite unexpected since the porphyrin ring in the corresponding nickel(II) tetramethylporphyrin  $[\text{Ni}(\text{TMeP})]$  is reported to be planar or nearly planar.<sup>11-13</sup> In the isopropyl complex, where the porphyrin ring is supposed to be highly deformed,<sup>14</sup> splitting of the *meso*  $\alpha$ -protons was observed at much higher temperature,  $+17\text{ }^{\circ}\text{C}$ . Thus, the activation free energy was estimated as  $56\text{ kJ mol}^{-1}$  at this temperature. These results suggest that the nonplanarity of the porphyrin ring greatly affects the rate of rotation of the coordinated imidazole ligand.

One of the problems in studying the hindered rotation of the axial ligands in iron(III) porphyrin system is the concomitant occurrence of the ligand dissociation. In fact, we have already pointed out that the dynamic process of the axial ligand in  $[\text{Fe}(\text{TMP})(2\text{-}^i\text{PrIm})_2]\text{Cl}$  includes both ligand rotation and ligand dissociation processes.<sup>5</sup> Thus, the activation free energy for ligand rotation in this complex is expected to be larger than the experimentally obtained value,  $57\text{ kJ mol}^{-1}$  at  $14\text{ }^{\circ}\text{C}$ . In contrast to the imidazole-iron(III) bond, the imidazole-cobalt(III) bond is known to be much stronger; the rate constant for ligand dissociation in  $[\text{Fe}(\text{TMP})(2\text{-MeIm})_2]\text{Cl}$  is larger than that of the corresponding cobalt(III) complex  $[\text{Co}(\text{TMP})(2\text{-MeIm})_2]\text{Cl}$  by the factor of ca.  $10^4$ .<sup>15</sup> Thus, the cobalt(III)-porphyrin complexes would be much more suitable than the corresponding iron(III)-porphyrin complexes to determine the activation free energies for the pure rotational process.

As an extension of the study on the metalloporphyrins with non-planar porphyrin ring,<sup>10,15-17</sup> we have examined how the barriers to imidazole rotation in  $[\text{bis}(\text{imidazole})(\text{meso-tetraalkylporphyrinato-cobalt(III)})\text{chloride } [\text{Co}(\text{TRP})(\text{L})_2]\text{Cl}$  change depending on the non-planarity of the porphyrin ring. These complexes are quite suitable to understand the relationship between the barriers to ligand rotation and the porphyrin nonplanarity because we can control the nonplanarity of the porphyrin ring by introducing the alkyl substituents with various bulkiness at the *meso* positions. The complex with unhindered imidazole  $[\text{Co}(\text{T}^i\text{PrP})(\text{HIm})_2]\text{Cl}$  and the *meso* unsubstituted complex with hindered imidazole  $[\text{Co}(\text{THP})(2\text{-}^i\text{PrIm})_2]\text{Cl}$  are also examined for comparison.



$[\text{Co}(\text{TRP})(\text{L})_2]\text{Cl}$

R = H, Me, Et,  $^i\text{Pr}$

L = 1-MeIm, 2-MeIm  
2-EtIm, 2- $^i\text{PrIm}$

## RESULTS

**UV-Visible Spectra:** In Table 1 are given the Soret and Q bands of a series of  $[\text{Co}(\text{TRP})(\text{L})_2]\text{Cl}$  taken in  $\text{CH}_2\text{Cl}_2$  at  $25\text{ }^{\circ}\text{C}$ .

**$^1\text{H}$  NMR Chemical Shifts at  $25\text{ }^{\circ}\text{C}$ :** In Table 2 are given the  $^1\text{H}$  NMR chemical shifts of a series of  $[\text{Co}(\text{TRP})(\text{L})_2]\text{Cl}$  taken in  $\text{CD}_2\text{Cl}_2$  or  $\text{CDCl}_3$  at  $25\text{ }^{\circ}\text{C}$ . While the pyrrole protons in the methyl and ethyl complexes as well as the unsubstituted complexes gave a singlet at this temperature, those in the isopropyl complexes  $[\text{Co}(\text{T}^i\text{PrP})(\text{L})_2]\text{Cl}$  with the bulky imidazole ligands generally showed multiplet. The same is true for the *meso*  $\alpha$ - and  $\beta$ -protons; the *meso*  $\alpha$ -protons of the isopropyl complexes showed complicated multiplet centered at ca. 4.5 ppm and the *meso*  $\beta$ -protons exhibited clearly separated signals at ca. 2.0 ppm. As a typical example, the  $^1\text{H}$  NMR spectrum of  $[\text{Co}(\text{T}^i\text{PrP})(2\text{-EtIm})_2]\text{Cl}$  is given in Figure 1. This complex showed exceptionally well-resolved pyrrole signals, two singlets and an AB quartet, as shown in the inset(a) of Figure 1.

**Temperature Dependent NMR Spectra:** When the temperature was lowered, every *meso* tetraalkyl-

porphyrin complex with bulky imidazole ligands showed splitting of the signals. In the inset(b) of Figure 1 is given the temperature dependent isopropyl methine signals of  $[\text{Co}(\text{T}^i\text{PrP})(2\text{-EtIm})_2]\text{Cl}$  under the irradiation of the isopropyl methyl signals at 1.9 ppm. The methine signals, which gave two singlets at 0 °C, clearly showed the coalescence and became a single line at higher temperature. In the case of the less bulky imidazole, no splitting of the signal was observed even at -72 °C as was revealed from the temperature dependent NMR spectra of  $[\text{Co}(\text{T}^i\text{PrP})(\text{HIm})_2]\text{Cl}$ . Similarly, no splitting was observed in the unsubstituted complex even if the axial ligand is bulky 2-<sup>i</sup>PrIm.

**Activation Free Energies for Ligand Rotation:** The activation free energies for ligand rotation, determined from the coalescence phenomena of the *meso*  $\alpha$ - and/or  $\beta$ -proton signals, are given in Table 3 together with those of the corresponding tetraarylporphyrin system. In  $[\text{Co}(\text{TMeP})(\text{L})_2]\text{Cl}$ , the *meso* methyl signal changed from a singlet to two singlets as the temperature was lowered. In the case of  $[\text{Co}(\text{TEtP})(\text{L})_2]\text{Cl}$ , the *meso* methylene protons also changed from a singlet to two singlets, although they should change from a

**Table 1.** UV-Visible Spectral Data in  $\text{CH}_2\text{Cl}_2$  at 25 °C ( $\lambda$  nm)

| R               | L                    | Soret | Q1  | Q2  |
|-----------------|----------------------|-------|-----|-----|
| H               | 2- <sup>i</sup> PrIm | 412   | 531 |     |
| Me              | 1-MeIm               | 435   | 556 | 602 |
| Me              | 2-MeIm               | 441   | 569 | 612 |
| Me              | 2-EtIm               | 441   | 567 | 612 |
| Me              | 2- <sup>i</sup> PrIm | 437   | 565 | 610 |
| Et              | 1-MeIm               | 436   | 558 | 600 |
| Et              | 2-MeIm               | 441   | 567 | 610 |
| Et              | 2-EtIm               | 441   | 566 | 609 |
| Et              | 2- <sup>i</sup> PrIm | 440   | 566 | 608 |
| <sup>i</sup> Pr | 1-MeIm               | 444   | 567 | 615 |
| <sup>i</sup> Pr | 2-MeIm               | 452   | 578 | 620 |
| <sup>i</sup> Pr | 2-EtIm               | 449   | 576 | 619 |
| <sup>i</sup> Pr | 2- <sup>i</sup> PrIm | 448   | 574 | 616 |

**Table 2.** Chemical Shifts of a Series of  $[\text{Co}(\text{TRP})(\text{L})_2]\text{Cl}$  at 25 °C in  $\text{CD}_2\text{Cl}_2$  or  $\text{CDCl}_3$  Solution ( $\delta$  ppm)

| R               | L                    | Py-H                     | <i>meso</i>           |                          | Imidazole |                |               |       |      |
|-----------------|----------------------|--------------------------|-----------------------|--------------------------|-----------|----------------|---------------|-------|------|
|                 |                      |                          | $\alpha$ -H           | $\beta$ -H               | 1-H       | 2- $\alpha$ -H | 2- $\beta$ -H | 4-H   | 5-H  |
| H               | 2-MeIm               | 9.45                     | (9.91) <sup>1)</sup>  | —                        | 2)        | -2.87          | —             | -1.36 | 3.67 |
| H               | 2- <sup>i</sup> PrIm | 9.40                     | (10.02) <sup>1)</sup> | —                        | 2)        | -4.67          | -1.39         | -1.75 | 3.90 |
| Me              | 2-MeIm               | 9.47                     | 4.14                  | —                        | 2)        | -2.30          | —             | -0.24 | 4.27 |
| Me              | 2-EtIm               | 9.39                     | 4.12                  | —                        | 2)        | -2.69          | -0.97         | -0.50 | 3.96 |
| Me              | 2- <sup>i</sup> PrIm | 9.40                     | 4.09                  | —                        | 2)        | -3.87          | -1.22         | -0.63 | 4.05 |
| Et              | 2-MeIm               | 9.43                     | 4.42                  | 1.73                     | 2)        | -2.38          | —             | -0.40 | 4.03 |
| Et              | 2-EtIm               | 9.46                     | 4.44                  | 1.72                     | 2)        | -2.59, -2.73   | -0.97         | -0.49 | 4.17 |
| Et              | 2- <sup>i</sup> PrIm | 9.42                     | 4.46                  | 1.72                     | 10.5      | -3.90          | -1.11         | -0.65 | 4.21 |
| <sup>i</sup> Pr | H-Im                 | 9.35                     | 4.61                  | 1.92                     | 10.05     | —              | —             | 0.46  | 4.13 |
| <sup>i</sup> Pr | 2-MeIm               | 9.25, 9.30<br>9.34, 9.38 | 4.46, 4.56            | 1.75, 1.81<br>2.02, 2.10 | 10.16     | -2.25          | —             | -0.11 | 4.13 |
| <sup>i</sup> Pr | 2-EtIm               | 9.33, 9.35<br>9.37, 9.40 | 4.48<br>4.54          | 1.88, 1.91<br>1.93       | 9.47      | -2.41          | -0.75         | -0.13 | 4.45 |
| <sup>i</sup> Pr | 2- <sup>i</sup> PrIm | 9.43(m)                  | 4.60<br>4.70          | 2.02                     | 9.26      | -3.64          | -0.98         | -0.34 | 4.33 |

1) Chemical shift of the protons directly bonded to the *meso* carbons.

2) The signal was not found probably due to the broadening.

**Table 3.** Activation Free Energy ( $\text{kJ mol}^{-1}$ ) at Coalescence Temperature. Value in the Parenthesis is a Coalescence Temperature.

| L                    | TPP <sup>1)</sup> | TMP <sup>1)</sup> | TRP <sup>2)</sup> |  |                             |                                   |
|----------------------|-------------------|-------------------|-------------------|--|-----------------------------|-----------------------------------|
|                      |                   |                   | R = Me            | R = Et   | R = <sup>i</sup> Pr         | R = <sup>t</sup> Bu <sup>3)</sup> |
| 1-MeIm               | <42 (<-72 °C)     | <42 (<-72 °C)     | —                 | —  | <42 (<-72 °C) <sup>4)</sup> | 57                                |
| 2-MeIm               | <42 (-72 °C)      | 60 (6.0 °C)       | 49 (-35 °C)       | 51 (-27 °C) <sup>5)</sup><br>49 (-40 °C) <sup>6)</sup> | 70 (57 °C)                  | —                                 |
| 2-EtIm               | <42 (-72 °C)      | 67 (30.8 °C)      | 52 (-40 °C)       | 53 (-15 °C)  | 73 (65 °C)                  | —                                 |
| 2- <sup>i</sup> PrIm | <42 (-72 °C)      | >88 (>130 °C)     | 58 (5 °C)         | 62 (30 °C)   | >77 (>70 °C)                | —                                 |

1) Reference 18. 2) This work. 3) Reference 27. 4) L = HIm. 5) Obtained from  $\beta$ -CH<sub>3</sub>. 6) Obtained from  $\alpha$ -CH<sub>2</sub>

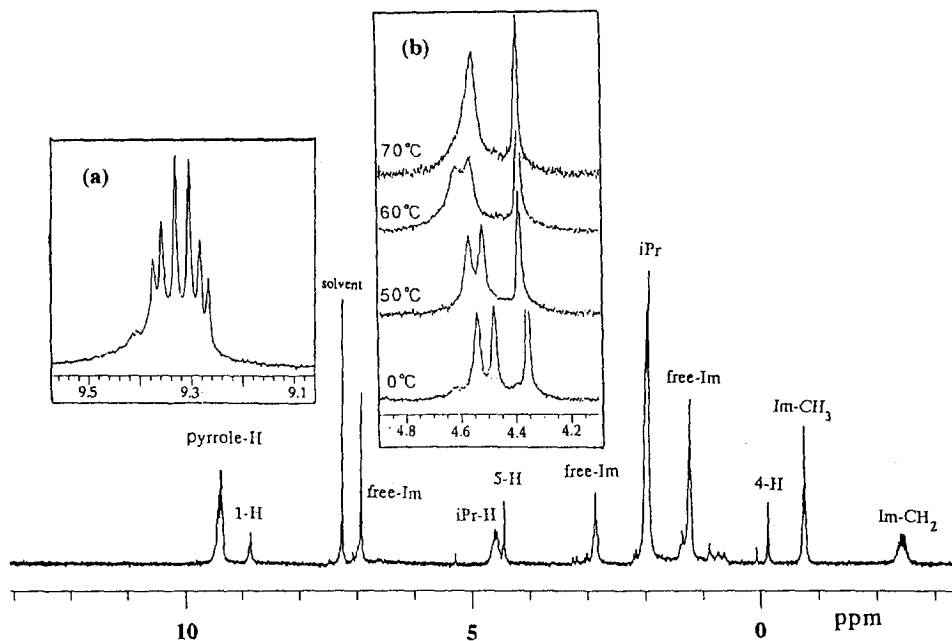


Figure 1.  $^1\text{H}$  NMR spectrum of  $[\text{Co}(\text{T}^i\text{PrP})(2\text{-EtIm})_2]\text{Cl}$  taken in  $\text{CDCl}_3$  at  $25^\circ\text{C}$ . Inset (a) is the pyrrole proton region showing two singlets and an AB quartet. Inset (b) is the temperature dependence of the isopropyl methine signals under the irradiation of the neighboring methyl protons.

singlet to two AB quartets. This must be due to the small difference in chemical shifts of the methylene protons in the homotopic ethyl groups. The *meso* methyl protons showed no splitting even at  $-72^\circ\text{C}$ , although the change from a singlet to two singlets is expected theoretically under the irradiation of the methylene protons. The result is ascribed to the small difference in chemical shifts of the diastereotopic methyl protons in  $[\text{Co}(\text{TEtP})(2\text{-MeIm})_2]\text{Cl}$  and  $[\text{Co}(\text{TEtP})(2\text{-}^i\text{PrIm})_2]\text{Cl}$ . Thus, the activation free energies were determined from the coalescence phenomena of the  $\alpha$ -methylene signals. In the case of  $[\text{Co}(\text{TEtP})(2\text{-EtIm})_2]\text{Cl}$ , however, even the methyl signals showed coalescence phenomena. Thus, the activation free energies were determined by using two different probes; the values obtained from the methyl and methylene signals were  $51\text{ kJ mol}^{-1}$  ( $-27^\circ\text{C}$ ) and  $49\text{ kJ mol}^{-1}$  ( $-40^\circ\text{C}$ ), respectively, at the coalescence temperature given in the parenthesis. In the case of  $[\text{Co}(\text{T}^i\text{PrP})(\text{L})_2]\text{Cl}$ , the *meso*  $\alpha$ -methine signal changed from a singlet to two singlets under the irradiation of the *meso* methyl signals. The *meso*  $\beta$ -methyl protons showed four sets of doublet in  $[\text{Co}(\text{T}^i\text{PrP})(2\text{-MeIm})_2]\text{Cl}$  and three sets of doublet in  $[\text{Co}(\text{T}^i\text{PrP})(2\text{-EtIm})_2]\text{Cl}$  even at room temperature. In the case of  $[\text{Co}(\text{T}^i\text{PrP})(2\text{-}^i\text{PrIm})_2]\text{Cl}$ , however, the  $\beta$ -methyl protons gave an unresolved signal even at low temperature. Rate constants and activation free energies for ligand rotation at the coalescence temperature were obtained by using conventional equations.

As mentioned, each proton showed sharp singlet even at  $-72^\circ\text{C}$  in the case of  $[\text{Co}(\text{T}^i\text{PrP})(\text{HIm})_2]\text{Cl}$ . If we assume that the chemical shift difference of the isopropyl methine protons is 10 Hz and the coalescence temperature is  $-80^\circ\text{C}$ , the activation free energy is calculated to be  $42\text{ kJ mol}^{-1}$ . If we assume that the chemical shift difference is 30 Hz, which is the case in  $[\text{Co}(\text{T}^i\text{PrP})(2\text{-MeIm})_2]\text{Cl}$ , and the coalescence temperature is  $-90^\circ\text{C}$ , then the activation free energy decreases to  $37\text{ kJ mol}^{-1}$ . Thus, the activation free energy of  $[\text{Co}(\text{T}^i\text{PrP})(\text{HIm})_2]\text{Cl}$  is described as  $< 42\text{ kJ mol}^{-1}$  in Table 3.

## DISCUSSION

**Stable Conformation in Solution:** Several examples have already been reported on the hindered rotation of the coordinated imidazole ligands in low spin iron(III) and cobalt(III) porphyrin complexes.<sup>5,18,19</sup> In the *meso* tetrasubstituted porphyrin system, the stable conformation was reported to be the one where the coordinated imidazole ligands are placed along the diagonal  $C_{\text{meso}}-M-C_{\text{meso}}$  axes above and below the porphyrin ring perpendicularly to each other as shown in Figure 2(a).<sup>7,8</sup> In the case of dodecasubstituted porphyrin complex such as bis(pyridine)(2,3,7,8,12,13,17,18-octaethyl-5,10,15,20-tetraphenylporphyrinatocobalt(III)), the stable conformation was reported to be the one in which the coordinated pyridine ligands are orientated along the diagonal N-Co-N axis as shown in Figure 2(b).<sup>19</sup> In the present case, the splitting pattern of the *meso*  $\alpha$ - and  $\beta$ -proton signals reveals that the stable conformation is the one given in Figure 2(a). Unambiguous evidence supporting this idea was obtained from the low temperature <sup>1</sup>H NMR spectra of [Co(TMeP)(L)<sub>2</sub>]Cl and [Co(T<sup>i</sup>PrP)(2-MeIm)<sub>2</sub>]Cl. The former gave two singlets and the latter gave four sets of doublet for the *meso* methyl protons when the ligand rotation was hindered on the NMR time scale. Although pyrrole protons of these complexes should give two singlets and an AB quartet if they take the conformation given in Figure 2(a), the chemical shifts are, in many cases, too close to observe this type of splitting. Exceptional cases are [Co(T<sup>i</sup>PrP)(2-MeIm)<sub>2</sub>]Cl and [Co(T<sup>i</sup>PrP)(2-EtIm)<sub>2</sub>]Cl in which the chemical shifts of the pyrrole protons are different enough to give this splitting pattern as shown in the inset (a) of Figure 1. Based on these observations, we concluded that the stable conformation is the one given in Figure 2(a).

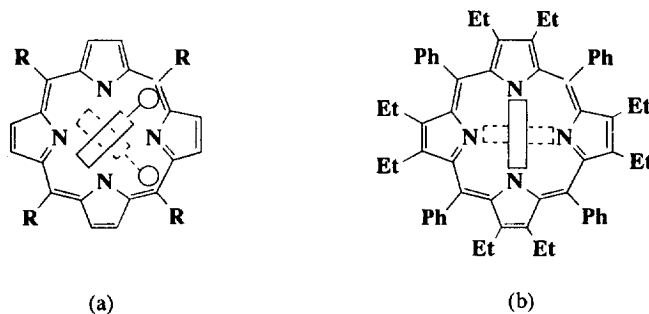


Figure 2. Stable conformations of (a) tetraalkylporphyrinatocobalt(III) with bulky imidazole ligands and (b) dodecasubstituted porphyrinatocobalt(III) with pyridine ligands.

**Nonplanarity of the Porphyrin Ring:** The data in Table 1 clearly indicate that both the Soret and Q bands are red shifted as the *meso* substituent becomes bulky; Soret band of [Co(TRP)(2-<sup>i</sup>PrIm)<sub>2</sub>]Cl varied from 412 nm (R = H) to 437 nm (R = Me) and 440 nm (R = Et), and then to 448 nm (R = <sup>i</sup>Pr). The Q1 band also moved from 531 to 565 and 566, and then to 574 nm for the H, Me, Et, and <sup>i</sup>Pr complexes, respectively. Thus, the order of the red shift is H  $\ll$  Me  $\leq$  Et  $<$  <sup>i</sup>Pr. The red shift was also observed in both the Soret and Q bands when 1-MeIm was replaced by much bulkier 2-MeIm. It was reported that the Soret and Q bands exhibit red-shift, when the porphyrin ring deforms, due to much larger destabilization of the HOMO relative to the LUMO.<sup>20-22</sup> Thus, the data in Table 1 indicate that the porphyrin ring deformation takes place in solution as the alkyl substituents are introduced at the *meso* and imidazole 2-positions.

Recent systematic studies on the structure of a series of nickel(II) *meso*-tetrasubstituted porphyrin

complexes [Ni(TRP)] by the molecular mechanics calculation and in some cases by the X-ray crystallographic analysis have also revealed that the  $S_4$  deformation of the porphyrin ring increases as the *meso* substituents become bulky.<sup>23</sup> This study has shown that the ruffling dihedral angle, which is defined by the dihedral angle between pyrrole rings in the diagonal positions and is indicating the degree of deformation of the porphyrin ring, changes from 25.3 and 21.0° in the Me and Et complexes to 36.6° in the <sup>i</sup>Pr complex. Since the unsubstituted complex [Ni(THP)] has been reported to have a planar porphyrin ring, the ruffling dihedral angle should be 0°.<sup>24</sup> Thus, the order of the ruffling dihedral angles is  $H \ll Et \leq Me < {}^iPr$ , which is in good agreement with the order of the red shift.

The <sup>1</sup>H NMR chemical shifts of these complexes also suggest the nonplanarity of the porphyrin ring in solution. For example, the imidazole methyl signals in a series of 2-MeIm complexes [Co(TRP)(2-MeIm)<sub>2</sub>]Cl were observed at -2.87, -2.30, -2.38, and -2.25 ppm for R = H, Me, Et, and <sup>i</sup>Pr, respectively. Thus, the methyl signal moves to lower magnetic field as the *meso* substituents become bulkier. Similar results were obtained for the imidazole 2- $\alpha$ -proton signals in a series of [Co(TRP)(2-<sup>i</sup>PrIm)<sub>2</sub>]Cl; the chemical shifts of these signals were -4.67, -3.87, -3.90, and -3.64 ppm for the complexes with R = H, Me, Et, and <sup>i</sup>Pr, respectively. Thus, the low field shift of up to 1.0 ppm was observed when the alkyl substituent was introduced at the *meso* positions. The imidazole 4-H signal also moved from -1.75 (R = H) to -0.34 ppm (R = <sup>i</sup>Pr). Even the imidazole 5-H signal moved from 3.90 (R = H) to 4.33 (R = <sup>i</sup>Pr). The downfield shift of the imidazole protons in the complexes with bulky alkyl substituent could be explained by the decrease in ring current caused by the deformation of the porphyrin ring, although recent study on the porphyrin ring current suggests that the decrease in ring current due to the nonplanarity of the porphyrin ring is ca. 5% even in a highly deformed porphyrin complex.<sup>25</sup> Since the imidazole 2- $\alpha$ -H and 4-H are located quite close to the *meso* substituents, the chemical shifts must be influenced not only by the ring current but by the steric factor. Thus, it might be safe to consider the downfield shift of 0.43 ppm observed in the imidazole 5-H as the reflection of the decrease in ring current due to the nonplanarity of the porphyrin ring. In both [Co(TRP)(2-MeIm)<sub>2</sub>]Cl and [Co(TRP)(2-<sup>i</sup>PrIm)<sub>2</sub>]Cl, the order of the downfield shift is  $H \ll Me \leq Et < {}^iPr$  which is again consistent with the UV-Vis results.

**Barriers to Rotation of the Imidazole Ligands:** The data in Table 3 indicate that the activation free energies of the complexes with bulky imidazole increase as the *meso* substituent changes from Me, Et, and then to <sup>i</sup>Pr group. Splitting of the signal was not observed, however, in the complexes which have no substituents at position 2 of the imidazole ring, as is clear from the low temperature NMR spectra of [Co(<sup>Ti</sup>PrP)(H-Im)<sub>2</sub>]Cl. No splitting of the signal was observed in the *meso* unsubstituted complex even if the axial ligand is bulky 2-<sup>i</sup>PrIm. Thus, in the present system, existence of substituents at both the *meso* positions and imidazole 2-position seems to be necessary for the observation of the hindered rotation on the NMR time scale at easily accessible temperature.

The high barriers to rotation observed in this system is interpreted as follows. In the presence of bulky substituents such as isopropyl group at the *meso* positions, porphyrin ring can no longer be planar as is clear from the X-ray crystallographic result of the analogous [Ni(<sup>Ti</sup>PrP)]; this porphyrin is highly  $S_4$  deformed and the average deviation of the *meso* carbons from the porphyrin mean plane reaches as much as 0.72 Å.<sup>14</sup> When bulky 2-MeIm binds to the cobalt to form [Co(<sup>Ti</sup>PrP)(2-MeIm)<sub>2</sub>]Cl, the ligand is orientated parallel to the porphyrin cavities as shown in A of Figure 3. Repulsive interaction between the ligand and *meso* substituent would be effectively weakened by the further ruffling of the porphyrin ring. Rotation of both of the imidazole ligands would increase the energy level and lead to the transition state of the rotation process. If we assume that the perpendicular conformations **T**<sub>1</sub> and **T**<sub>2</sub> in Figure 3, where the imidazole ligands are placed along the diagonal N-Co-N axes, are the transition states, the energy level of these states would be greatly increased due to the severe steric repulsion between the imidazole ring and the porphyrin core. It should be noted that the

conformation of the porphyrin ring changes concomitantly as the axial ligands rotate. Further rotation of the imidazole ligands leads to the stable conformations, **B** and **C**. Figure 3 shows that the porphyrin ring inversion takes place during the rotation process from **A** to **B** or from **A** to **C**. Introduction of much bulkier substituent at position 2 of the imidazole ring would destabilize both the ground state and transition state. While the repulsive interaction in the ground state is expected to be weakened effectively by the much deeper  $S_4$  ruffling of the porphyrin ring, the energy relief must be smaller at the transition state where the steric repulsions between *meso* substituents and the pyrrole  $\beta$ -hydrogens increase. In fact, the activation free energy increased from 51 kJ mol<sup>-1</sup> in [Co(TEtP)(2-MeIm)<sub>2</sub>]Cl to 62 kJ mol<sup>-1</sup> in [Co(TEtP)(2-<sup>i</sup>PrIm)<sub>2</sub>]Cl.

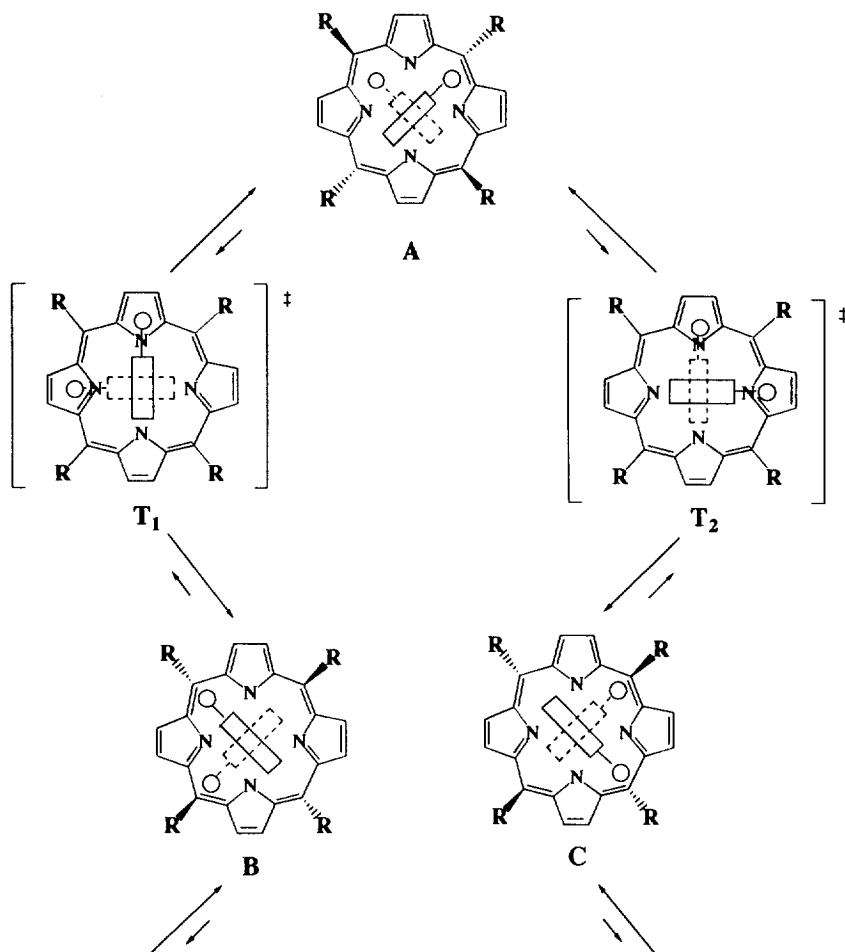


Figure 3. Schematic presentation of the rotation of the coordinated imidazole ligands in [Co(TRP)(L)<sub>2</sub>]Cl. **A**: Ground state conformation. The ligands are orientated along the diagonal  $C_{\text{meso}}\text{-Co-}C_{\text{meso}}$  axes.  $T_1$  and  $T_2$ : Plausible structure for the transition state of rotation where two ligand molecules are placed along the diagonal  $N\text{-Co-}N$  axes. **B** and **C**: Ground state conformations after the 90° rotation of both of the ligands.

Tetramethylporphyrin is known to be planar or nearly planar from the X-ray crystallographic analysis of the analogous [Ni(TMeP)].<sup>11-13</sup> Yet, the activation free energies for rotation in [Co(TMeP)(L)<sub>2</sub>]Cl were still fairly high, 49 to 58 kJ mol<sup>-1</sup> depending on the axial ligand. Consideration of the molecular model of this complex suggests that the energy difference between the ground and transition states would be quite small if the porphyrin ring maintains its planarity. Relatively high barrier to imidazole rotation suggests that the conformation of the porphyrin ring changes from the planar to the S<sub>4</sub> ruffled structure by the coordination of the bulky imidazole ligands. In fact, nonplanarity of this complex is suggested both by the red shift of the Soret and Q bands in the UV-Visible spectra and by the downfield shift of the imidazole signals in the <sup>1</sup>H NMR spectra as compared with those of the corresponding unsubstituted [Co(THP)(L)<sub>2</sub>]Cl. Thus, the structure of [Co(TMeP)(L)<sub>2</sub>]Cl would be quite similar to that of [Co(T<sup>i</sup>PrP)(L)<sub>2</sub>]Cl except for the degree of deformation. The best example supporting this speculation is the X-ray crystallographic structure of [Fe(TPP)(2-MeIm)<sub>2</sub>]<sup>+</sup>.<sup>26</sup> Although tetraphenylporphyrin (H<sub>2</sub>TPP) is a planar ligand, the porphyrin ring in [Fe(TPP)(2-MeIm)<sub>2</sub>]ClO<sub>4</sub> was reported to be S<sub>4</sub> ruffled due to the steric repulsion between bulky 2-MeIm and *o*-H of the *meso* phenyl groups; average deviation of the four *meso* carbons from the mean porphyrin plane was 0.40 Å. Similarly, the porphyrin ring in [Fe(TMP)(1,2-Me<sub>2</sub>Im)<sub>2</sub>]ClO<sub>4</sub> was reported to be highly S<sub>4</sub> ruffled in the crystal as mentioned in the INTRODUCTION of this paper.<sup>9</sup> The activation free energy for rotation of the 1,2-Me<sub>2</sub>Im ligand in this complex was reported to be 47 kJ mol<sup>-1</sup> at -34 °C.<sup>5</sup> These results suggest that, in order to observe the hindered ligand rotation on the NMR time scale at an easily accessible temperature, the porphyrin ring must be deformed to have deep cavities.

Based on the discussion given above and the rotation mechanism shown in Figure 3, the activation free energy for ligand rotation obtained by the dynamic NMR method ( $\Delta G_{\text{obsd}}^*$ ) thus includes the intrinsic energy required for the porphyrin ring inversion ( $\Delta G_{\text{inv}}^*$ ) and some additional energy ( $\Delta G^*$ ) related with the rotation of imidazole ligands as presented by equation (1). In this equation, the first term  $\Delta G_{\text{inv}}^*$  indicates the

$$\Delta G_{\text{obsd}}^* = \Delta G_{\text{inv}}^* + \Delta G^* \quad (1)$$

difference in the conformational energies of the porphyrin ring between the ground state A and the transition state T<sub>1</sub> or T<sub>2</sub>. The second term  $\Delta G^*$  includes every additional energy caused by the presence of the axial ligands. The major part of  $\Delta G^*$  must be the steric repulsion of the imidazole ligands with the porphyrin core at the transition state for rotation. The first term is expected to predominate in the tetraalkylporphyrin system such as [Co(T<sup>i</sup>PrP)(2-MeIm)<sub>2</sub>]Cl since the severe steric repulsion takes place between the *meso* <sup>i</sup>Pr and pyrrole β-hydrogen at the transition state as compared with the ground state. In contrast, the second term might be predominant in the tetraarylporphyrin system such as [Co(TMP)(2-MeIm)<sub>2</sub>]Cl due to the steric repulsion between imidazole 2-substituent and the porphyrin nitrogens at the transition state.<sup>18</sup>

Quite recently, Meforth *et al.* reported the hindered rotation of the unhindered ligands in highly nonplanar porphyrins such as 2,3,7,8,12,13,17,18-octaethyl-5,10,15,20-tetraphenylporphyrinatocobalt(III) and *meso*-tetra(*t*-butyl)porphyrinatocobalt(III) systems.<sup>27</sup> The porphyrin ring of the former complex is S<sub>4</sub> saddled and that of the latter complex is S<sub>4</sub> ruffled. In both systems, the porphyrin rings have very deep cavities and the ligand molecules bind along the cavities, making the perpendicular alignment above and below the porphyrin ring. In these systems, even the rotation of less bulky ligands such as 3-chloropyridine and 1-methylimidazole was hindered on the NMR time scale. The activation free energy for ligand rotation in [Co(T<sup>t</sup>BuP)(1-MeIm)<sub>2</sub>]Cl was estimated to be 57 kJ mol<sup>-1</sup>. Since the activation energy for the porphyrin ring inversion in this system is expected to be quite large due to the highly S<sub>4</sub> ruffled structure, the major part of the activation energy for the ligand rotation process in [Co(T<sup>t</sup>BuP)(1-MeIm)<sub>2</sub>]Cl would be ascribed to the conformational change of the porphyrin ring during the rotation of the imidazole ligands.



In conclusion, we have found that the activation free energy for ligand rotation in a series of tetraalkylporphyrinatocobalt(III) complexes,  $[\text{Co}(\text{TRP})(\text{L})_2]\text{Cl}$  where R = H, Me, Et, or <sup>i</sup>Pr and L is substituted imidazole such as 1-MeIm, 2-MeIm, 2-EtIm, or 2-<sup>i</sup>PrIm, increases as the *meso* and/or imidazole 2-substituent become bulky. The increase in activation free energy has been ascribed to the nonplanarity of the porphyrin ring caused by the steric repulsion of the *meso* substituent with pyrrole β-hydrogens and with imidazole 2-substituent based on the red shifted Soret and Q bands in the UV-Visible spectra and the downfield-shifted imidazole protons in the <sup>1</sup>H NMR spectra.

**Acknowledgement:** The authors thank Professor Michiko Iwamura, Dr. Toshiaki Furuta, and Dr. Soichiro Watanabe (Department of Biomolecular Science, Faculty of Science, Toho University) for NMR measurement. The authors also thank Prof. Saburo Neya of Kyoto Pharmaceutical University for various information on the synthesis of tetraalkylporphyrins. This work was supported by a Grant in Aid for Scientific Research (No. 07640732) from Ministry of Education, Science, Sports and Culture of Japan.

## EXPERIMENTAL

**General:** Pyrrole, acetaldehyde, propionaldehyde, isobutylaldehyde were purchased and they were distilled before use. <sup>1</sup>H NMR spectra were recorded either on a JEOL GX270 operating at 270 MHz or on a JEOL LA300 operating at 300 MHz. Chemical shifts were referenced to residual  $\text{CH}_2\text{Cl}_2$  ( $\delta = 5.32$  ppm) or  $\text{CHCl}_3$  ( $\delta = 7.26$ ). UV-Visible spectra were recorded on a Hitachi 200-10 spectrophotometer at 25 °C using  $\text{CH}_2\text{Cl}_2$  as solvent. The activation free energies for the ligand rotation were obtained by the dynamic <sup>1</sup>H NMR method.<sup>28,29</sup> The rate constant ( $k_c$ ;  $\text{s}^{-1}$ ) for ligand rotation at the coalescence temperature ( $T_c$ ; K) was calculated by using the following equation, where  $\Delta\nu$  (Hz) is the difference in chemical shift of the exchanging protons in the slow limit. The activation free energies for the ligand rotation ( $\Delta G_c^\ddagger$ ;  $\text{kJ mol}^{-1}$ ) was then calculated by the Eyring's equation.

$$k_c = (\pi \Delta\nu)/(2)^{1/2}$$

**Synthesis:** A series of tetraalkylporphyrins were prepared from freshly distilled pyrrole and the corresponding aldehyde in propionic acid at 90 °C according to Neya's method.<sup>17,30,31</sup> Insertion of cobalt was carried out in refluxed  $\text{CHCl}_3$ - $\text{CH}_3\text{OH}$ (3:1) using excess amount of  $\text{CoCl}_2$ . The cobalt(II) complexes  $[\text{Co}(\text{TRP})]$  thus obtained were purified by chromatography on alumina. The chloroform solution of the purified cobalt(II) complex was stirred overnight with excess imidazole under air to form bis(imidazole) complex  $[\text{Co}(\text{TRP})(\text{L})_2]\text{Cl}$ . The green-purple solid, obtained after the chromatography on neutral alumina with  $\text{CH}_2\text{Cl}_2$ - $\text{CH}_3\text{OH}$ (95:5), was purified by recrystallization from  $\text{CH}_2\text{Cl}_2$ -hexane. The UV-Visible and <sup>1</sup>H NMR data of these complexes are given in Table 1 and Table 2, respectively.

## REFERENCES

1. W. R. Scheidt, D. M. Chipman, *J. Am. Chem. Soc.* **1986**, *108*, 1163-1167.
2. F. A. Walker, B. H. Huynh, W. R. Scheidt, S. R. Osvath, *J. Am. Chem. Soc.* **1986**, *108*, 5288-5297.
3. Y. Yamamoto, N. Nanai, R. Chujo, T. Suzuki, *FEBS Lett.*, **1990**, *264*, 113-116
4. M. J. M. Nasset, N. V. Shokhirev, P. D. Enemark, S. E. Jacobson, F. A. Walker, *Inorg. Chem.* **1996**, *35*, 5188-5200.
5. M. Nakamura, K. Tajima, K. Tada, K. Ishizu, N. Nakamura, *Inorg. Chim. Acta* **1994**, *224*, 113-124.

6. M. Nakamura, J. T. Groves, *Tetrahedron* **1988**, *44*, 3225-3230.
7. F. A. Walker, U. Simonis, *J. Am. Chem. Soc.* **1991**, *113*, 8652-8657.
8. M. Nakamura, N. Nakamura, *Chem. Lett.* **1991**, 1885-1888.
9. O. Q. Munro, H. M. Marques, P. G. Debrunner, K. Mohanrao, W. R. Scheidt, *J. Am. Chem. Soc.* **1995**, *117*, 935-954.
10. M. Nakamura, T. Ikeue, S. Neya, N. Funasaki, N. Nakamura, *Inorg. Chem.* **1996**, *35*, 3731-3732.
11. J. C. Gallucci, P. N. Sweptston, J. A. Ibers, *Acta Crystallogr.* **1982**, *38*, 2134.
12. F. W. Kutzler, P. N. Sweptston, Z. B. Yellin, D. E. Ellis, J. A. Ibers, *J. Am. Chem.Soc.* **1983**, *105*, 2996-3004.
13. T.P. Newcomb, M.R. Godfrey, B.M. Hoffman, J.A. Ibers, *J. Am. Chem. Soc.* **1989**, *111*, 7078-7084.
14. T. Ema, M. O. Senge, N. Y. Nelson, H. Ogoshi, K. M. Smith, *Angew. Chem. Int. Ed. Engl.* **1994**, *33*, 1879-1881.
15. M. Nakamura, *Bull. Chem. Soc. Jpn* **1995**, *68*, 197-203.
16. M. Nakamura, Y. Kawasaki, *Chem. Lett.* **1996**, 805-806.
17. M. Nakamura, T. Ikeue, H. Fujii, T. Yoshimura, *J. Am. Chem. Soc.*, *in press*, **1997**.
18. M. Nakamura, A. Ikezaki, *Chem. Lett.* **1995**, 733-734.
19. C. J. Medforth, C. M. Muzzi, K. M. Smith, R. J. Abraham, J. D. Hobbs, J. A. Shelnut, *J. Chem. Soc. Chem. Commun.* **1994**, 1843-1844.
20. K. M. Barkigia, L. Chantrunpong, K. M. Smith, J. Fajer, *J. Am. Chem. Soc.* **1988**, *110*, 7566-7567.
21. T. Takeuchi, H. B. Gray, W. A. Goddard III, *J. Am. Chem. Soc.* **1994**, *116*, 9730-9732.
22. M. O. Senge, T. Ema, K. M. Smith, *J. Chem. Soc. Chem. Commun.* **1995**, 733-734.
23. W. Jentzen, M. C. Simpson, J. D. Hobbs, X. Song, T. Ema, N. Y. Nelson, C. J. Medforth, K. M. Smith, M. Veyrat, M. Mazzanti, R. Ramasseul, J. -C. Marchon, T. Takeuchi, W. A. Goddard, III, J. A. Shelnut, *J. Am. Chem. Soc.* **1995**, *117*, 11085-11097.
24. W. Jantzen, I. T. Tyrk, W. R. Scheidt, J. A. Schelnutt, *Abstract of 210th ACS Natioal Meeting, Inorg. Division*, 531, Chicago, **1995**.
25. C. J. Medforth, C. M. Muzzi, K. M. Shea, K. M. Smith, R. J. Abraham, S. Jia, J. A. Shelnut, *J. Chem. Soc. Perkin 2*, **1997**, 839-844.
26. W. R. Scheidt, J. F. Kirner, J. L. Hoard, C. A. Reed, *J. Am. Chem. Soc.* **1987**, *109*, 1963-1968.
27. C. J. Medforth, C. M. Muzzi, K. M. Shea, K. M. Smith, R. J. Abraham, S. Jia, J. A. Shelnut, *J. Chem. Soc. Perkin 2*, **1997**, 833-837.
28. M. Oki, *Application of Dynamic NMR Spectroscopy to Organic Chemistry*, VCH, Deerfield, FL, **1985**.
29. J. Sandstrom, *Dynamic NMR Spectroscopy*, Academic Press, London, **1982**.
30. S. Neya, H. Yodo, N. Funasaki, *J. Heterocyclic Chem.* **1993**, *30*, 549-550.
31. S. Neya, N. Funasaki, *J. Heterocyclic Chem.* **1997**, *34*, 689-690.

(Received in Japan 6 June 1997; accepted 9 July 1997)